

## Disturbance rejection program induced by strap-down seeker time delay

Wang Wei, Lin Defu, Xu Ping

(School of Aerospace Engineering, Beijing Institute of Technology, Beijing 100081, China)

**Abstract:** The disturbance rejection rate problem caused by strap-down seeker was studied, the parasitical loop model induced by strap-down seeker time delay was established, the principium of how time delay causes disturbance rejection was analyzed, and the function of disturbance rejection rate induced by strap-down seeker time delay was deduced. Moreover, stability of the parasitical loop caused by time delay was investigated and of the parasitical loop with different guidance parameters was illustrated. The simulation result shows that, if the guidance system lag increases relatively to the missile aerodynamic time constant, the system can overcome larger seeker time delay; if the missile aerodynamic time constant is reduced, the guidance can tolerate larger seeker time delay. Disturbance rejection rate problem discussed in the paper is significant in the practical utilization.

**Key words:** strap-down seeker; disturbance rejection; parasitical loop

**CLC number:** TJ765 **Document code:** A **Article ID:** 1007-2276(2015)09-2854-04

## 捷联导引头延时引起的隔离度问题研究

王 伟, 林德福, 徐 平

(北京理工大学 宇航学院, 北京 100081)

**摘 要:** 研究了捷联导引头引起的隔离度问题, 建立了捷联导引头延时造成的寄生回路模型, 分析了捷联导引头延时引起隔离的机理, 得到了捷联导引头延时引起的隔离度函数。研究了导引头延时造成寄生回路的稳定性, 在制导参数取不同值情况下, 绘制捷联导引头延时引起的寄生回路稳定区域。仿真结果表明: 制导系统延迟环节动力学时间常数相对于弹体动力学时间常数越大, 对系统克服导引头延时的影响越有利。减小弹体气动力时间常数, 可以增强系统容忍导引头延时时间的能力。研究成果对于实现捷联导引头的工程应用具有重大意义。

**关键词:** 捷联导引头; 隔离度; 寄生回路

收稿日期: 2015-01-07; 修订日期: 2015-02-12

基金项目: 国家自然科学基金(61172182)

作者简介: 王伟(1984-), 男, 博士生, 主要从事飞行器总体设计、飞行器制导与控制方面的研究。Email: wangweiyh@bit.edu.cn

导师简介: 林德福(1971-), 男, 教授, 主要从事飞行器总体设计方面的研究。Email: lindf@bit.edu.cn

## 0 Introduction

To provide more accurate target information, the seeker, as a core guidance system measurement component, should implement complicated signal processing. The complicated signal processing, nevertheless, must consume a lot of time, inducing the time delay to the output signal of seeker. For traditional gimballed seekers, the time delay just increases the guidance system time constant and the guidance time. For strap-down seekers, however, the time delay causes the problem of disturbance rejection apart from that of the guidance system time constant. Focusing on the time delay of strap-down seeker, this paper mainly researches on the disturbance rejection problem.

### 1 Principium analysis of disturbance rejection problem with strap-down seeker time delay

The parasitical loop block model caused by the time delay of strap-down seeker is illustrated in Fig.1.  $q$  is the line-of-sight (LOS) angle,  $\varepsilon$  is the angle of seeker light axis with respect to the LOS,  $k_s$  is the calibration factor of staring strap-down seeker,  $\dot{q}_s$  is the output LOS angular rate,  $T_d$  is the time constant of differential network,  $1/(Ts+1)$  is the lag of guidance system,  $N$  is the navigation ratio of proportional navigation,  $v$  is the missile flight velocity,  $T_m$  and  $\mu_m$  are correspondingly the time constant and damping ratio of missile autopilot,  $T_a$  is the missile turning rate time constant,  $\vartheta_M$  is the missile attitude angle,  $k_g$  is the calibration factor of attitude gyro, and  $\tau$  is

the seeker time delay.

In Fig.1, missile body movement is coupled into seeker output signal of LOS angular rate through two channels: one is the missile disturbance channel and the other is compensation channel of attitude gyro. The detail coupling signals of the two channels will be discussed below:

(1) Coupling signal component  $\Delta \dot{q}_{s1}$  through missile disturbance channel is:

$$\Delta \dot{q}_{s1} = -\frac{e^{-\tau s}}{(T_d s + 1)^2} \dot{\vartheta}_M \tag{1}$$

(2) Coupling signal component  $\Delta \dot{q}_{s2}$  through missile attitude gyro compensation channel is:

$$\Delta \dot{q}_{s2} = -\frac{1}{(T_d s + 1)^2} \dot{\vartheta}_M \tag{2}$$

Therefore, the total seeker output LOS angular rate  $\Delta \dot{q}_s$  induced by missile movement:

$$\Delta \dot{q}_s = \frac{1 - e^{-\tau s}}{(T_d s + 1)^2} \dot{\vartheta}_M \tag{3}$$

Through Equ. (3), the seeker disturbance rejection function induced by time delay  $G_{is}(s)$  is:

$$G_{is}(s) = \frac{\Delta \dot{q}_{s1}}{\dot{\vartheta}_M} = \frac{1 - e^{-\tau s}}{(T_d s + 1)^2} \tag{4}$$

Through Equ. (4), if the time delay  $\tau$  is 0, missile movement would not be coupled into the seeker output signal of LOS angular rate. Therefore the Equ. (4) could be considered as the disturbance rejection function with the strap-down seeker time delay.

## 2 Parasitic loop stability analysis

As demonstrated in Fig.1, the close-loop characteristic

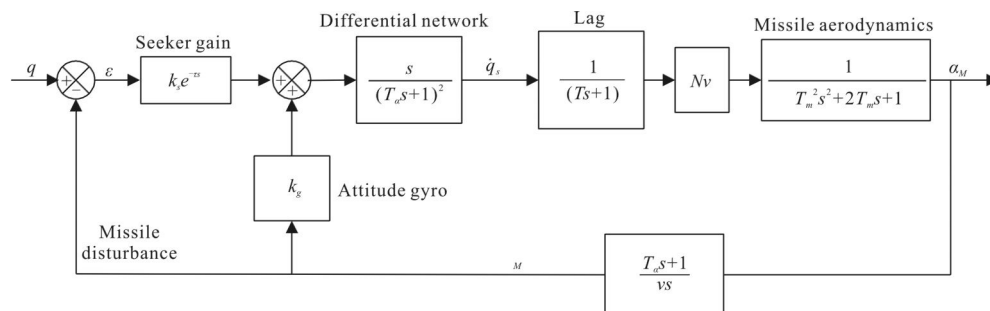


Fig.1 Parasitical loop induced by strap-down seeker time delay

equation of the parasitic loop caused by strap-down seeker is:

$$\frac{1}{e^{-\tau s}-1} + \frac{N(T_\alpha s+1)}{(T_d s+1)^2(Ts+1)(T_m^2 s^2+2\mu_m T_s+1)}=0 \quad (5)$$

Define the dimensionless quantities:

$$B_d = \frac{T_m}{T_d}, B = \frac{T_m}{T}, B_\alpha = \frac{T_m}{T_\alpha}, B_\tau = \frac{T_m}{\tau}, \bar{\omega} = T_m \omega,$$

$$\bar{a}_0 = \frac{T_d^2 T T_m^2}{T_m^5} = \frac{1}{B_d^2 B},$$

$$\bar{a}_1 = \frac{2\mu_m T_m T_d^2 T + T_m^2 (2T_d T + T_d^2)}{T_m^4} = \frac{2\mu_m}{B_d^2 B} + \frac{2}{B_d B} + \frac{1}{B_d^2},$$

$$\bar{a}_2 = \frac{T_d^2 T + 2\mu_m T_m (2T_d T + T_d^2) + T_m^2 (T + 2T_d)}{T_m^3} = \frac{2}{B_d B} +$$

$$\frac{1}{B_d^2} + 2\mu_m \left( \frac{1}{B} + \frac{2}{B_d} \right) + 1,$$

$$\bar{a}_3 = \frac{(2T_d T + T_d^2) + 2\mu_m T_m (T + 2T_d) + T_m^2}{T_m^2} = \frac{2}{B_d B} +$$

$$\frac{1}{B_d^2} + 2\mu_m \left( \frac{1}{B} + \frac{2}{B_d} \right) + 1,$$

$$\bar{a}_4 = \frac{(T + 2T_d) + 2\mu_m T_m}{T_m} = \frac{1}{B} + \frac{2}{B_d} + 2\mu_m,$$

$$\bar{a}_6 = \bar{a}_0 \bar{\omega}^5 - \bar{a}_4 \bar{\omega}^3 + \bar{a}_1 \bar{\omega}, \bar{a}_7 = \bar{a}_1 \bar{\omega}^4 - \bar{a}_3 \bar{\omega}^2 + 1,$$

$$\bar{a}_6 = \frac{N\bar{a}_7 + N\bar{a}_6 \frac{1}{B_\alpha} \bar{\omega}}{\bar{a}_7^2 + \bar{a}_6^2}, \bar{a}_9 = \frac{(N\bar{a}_7 \frac{1}{B_\alpha} \bar{\omega} - N\bar{a}_6)}{\bar{a}_7^2 + \bar{a}_6^2},$$

$$C_1 = \frac{\sin\left(\frac{1}{B_\tau} \bar{\omega}\right)}{2[1 - \cos\left(\frac{1}{B_\tau} \bar{\omega}\right)]},$$

So, the solution of system characteristic equation is:

$$B_\tau = \frac{\bar{\omega}}{\pi + 2\arcsin\left(\frac{2C_1}{\sqrt{4C_1^2 + 1}}\right)} \quad (6)$$

The stable region obtained by Equ. (6) is shown in Fig.2-5. Figure 2 plots the stable region defined by  $B_\tau$  versus  $B_d$  in condition of  $B_\alpha=0.05, B=2.5, \mu_m=0.7$ , and  $N$  at different values of 3, 4, 5. In the figure, the stable region decreases with  $B_d$  increasing, which means that with the seeker differential network faster than the missile aerodynamics, the guidance system could tolerate shorter seeker time delay. Moreover, the stable region decreases if the navigation ratio  $N$  increases, which reflects that the guidance system could tolerate shorter time delay with the guidance system bandwidth increasing. Fig.3 plots the stable region defined by  $B_\tau$  versus  $B_d$  in condition of  $B_\alpha =$

0.05,  $B=2.5, N=4$ , and  $\mu_m$  at different values of 0.1, 0.5, and 0.9. It can be obtained that the missile damping ratio  $\mu_m$  has heavy influence on the stable region from Fig.3.

The larger  $\mu_m$  is, the larger system stability becomes. Figure 4 plots the stability defined by  $B_\tau$  versus  $B_d$  in the condition of  $B_\alpha=0.05, N=4, \mu_m=0.7$ , at different values of 1, 2, and 3. In the figure, the stability decreases with  $B$ . So, if the guidance system lag increases relatively to the missile aerodynamic time constant, the system can overcome larger seeker time delay. Figure 5 plots the stable region defined by  $B_\tau$  versus  $B_d$  in condition of  $B =$

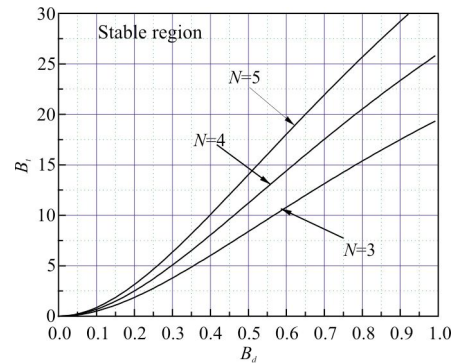


Fig.2 Stable region with  $N$  at 3, 4, and 5

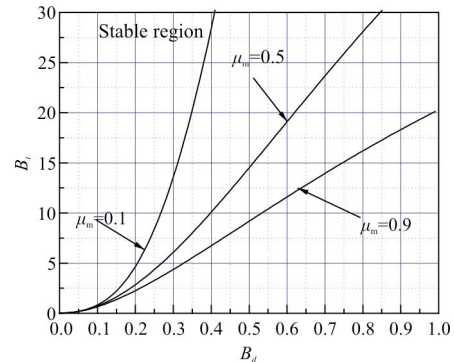


Fig.3 Stable region with  $\mu_m$  at 0.1, 0.5, and 0.9

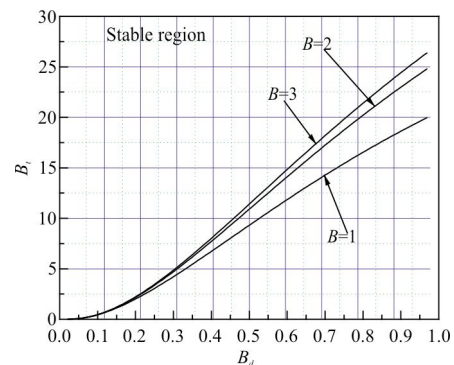


Fig.4 Stable region with  $B$  at 1, 2, 3

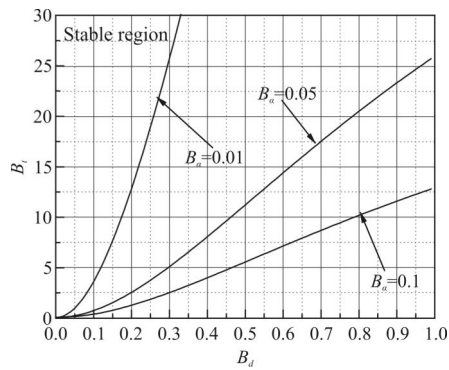


Fig.5 Stable region with  $B_\alpha$  at 0.01, 0.05, 0.1

2.5,  $N=4$ ,  $\mu_m=0.7$ , and  $B_\alpha$  at different values of 0.01, 0.05, and 0.1. In this figure, the stable region increases with  $B_\alpha$ , reflecting that if the missile aerodynamic time constant is reduced, the guidance can tolerate larger seeker time delay.

### 3 Conclusion

It is meaningful for China military industry to occupy the technology of strap-down seeker, which respects the development of seeker technology. The paper investigated

the disturbance rejection problem caused by strap-down seeker time delay and deduced the stable region of the parasitical loop caused by time delay. As one of the key problems of strap-down seeker, disturbance rejection rate problem discussed in the preceding sections is significant in the practical utilization.

### References:

- [1] Zhou Ruiqing, Liu Xinhua, Shi Shouxia, et al. Strap-down Seeker Stability and Track Technology[M]. Beijing: National Defence Industry Press, 2010. (in Chinese)
- [2] Captain Thomas, Callen R. Guidance law design for tactical weapons with strapDown seekers[C]//AIAA-79-1732.
- [3] Qi Zaikang, Xia Qunli. Guided Weapon Control System[M]. Beijing: Beijing Institute of Technology Press, 2003. (in Chinese)
- [4] Dong Jingxin, Zhao Changde, Xiong Shenshu, et al. Control Engineering Basic [M]. Beijing: Tsinghua University Press, 2003. (in Chinese)
- [5] Meng Xiuyun. Missile Guidance and Control System Principle[M]. Beijing: Beijing Institute of Technology, 2003. (in Chinese)

\*\*\*\*\*

(上接第 2853 页)

### 参考文献:

- [1] Tang Wei, Ye Dong. 3D computer vision measurement systems [J]. *Infrared and Laser Engineering*, 2008, 37 (S): 328-332. (in Chinese)
- [2] Xing Jichuan, Luo Xiaohong. Measurement of truck carriage volume with laser triangulation [J]. *Infrared and Laser Engineering*, 2012, 41(11): 3083-3087. (in Chinese)
- [3] Dai Shijie, Shao Meng, Wang Zhiping, et al. Study on the two-step method to remove the background in 3D measurement of titanium blade [J]. *Journal of Optoelectronics · Laser*, 2014, 25 (8): 1540-1547. (in Chinese)
- [4] Chen Yongquan, Zhao Jianke, Yuan Xianglan, et al. Study on absolute phase-unwrapping method [J]. *Infrared and Laser Engineering*, 2008, 37(S): 23-25. (in Chinese)
- [5] Towers C, Towers D, Zhang Z. Optical imaging of physical objects: US, 12/377180[P]. 2007-08-13.
- [6] Zhang Z, Ma H, Zhang S, et al. Simple calibration of a phase-based 3D imaging system based on uneven fringe projection[J]. *Optics Letters*, 2011, 36(5): 627-629.
- [7] Zhang Z, Towers C E, Towers D P. Uneven fringe projection for efficient calibration in high-resolution 3D shape metrology [J]. *Applied Optics*, 2007, 46(24): 6113-6119.
- [8] Zhang Z. Review of single-shot 3D shape measurement by phase calculation-based fringe projection techniques [J]. *Optics and Lasers in Engineering*, 2012, 50(8): 1097-1106.
- [9] Hao Yudong, Zhao Yang, Li Dacheng. Analysis of two-error in grating projection profilometry [J]. *Acta Optica Sinica*, 2000, 20(3): 376-379. (in Chinese)
- [10] Fu Y, Luo Q. Fringe projection profilometry base on a novel phase shift method [J]. *Optics Express*, 2011, 22 (19): 21739-21747.
- [11] Zhao H, Chen W, Tan Y. Phase-unwrapping algorithm for the measurement of three-dimensional object shapes [J]. *Applied Optics*, 1994, 33(20): 4497-4500.
- [12] Lei Zhihui, Li Jianbing. Full automatic phase unwrapping method based on projected double spatial frequency fringes [J]. *Acta Optica Sinica*, 2006, 26(1): 39-42. (in Chinese)